



# Interaction of sulfadiazine with cyclodextrins in aqueous solution and solid state

Alicia Delrivo, Ariana Zoppi, Marcela Raquel Longhi\*

Facultad de Ciencias Químicas, Universidad Nacional de Córdoba, Córdoba, Argentina

## ARTICLE INFO

### Article history:

Received 2 August 2011

Received in revised form

15 September 2011

Accepted 3 October 2011

Available online 18 October 2011

### Keywords:

Sulfadiazine

Complexation

Cyclodextrins

Nuclear magnetic resonance

Scanning electron microscopy

X-ray diffractometry

## ABSTRACT

The main objective of this work was to increase the solubility of sulfadiazine by formation of inclusion complexes with  $\beta$ -cyclodextrin, and methyl- $\beta$ -cyclodextrin. The apparent stability constants have been determined by phase solubility studies in water and buffer solutions of pH values of 2 and 8. The stoichiometry of all complexes was found to be 1:1 but different relative affinities were found for each cyclodextrin. It was possible to obtain a greater overall solubility by using a combined approach of pH adjustment and complexation with cyclodextrins. Guest–host interactions have been investigated using nuclear magnetic resonance. Complexes were prepared in solid state by different methods and were characterized using differential scanning calorimetry, thermogravimetric analysis, Fourier-transform infrared spectroscopy, X-ray diffractometry and scanning electron microscopy. The dissolution rate of the drug from the inclusion complex made by freeze-dried was much faster than this of the pure drug.

© 2011 Elsevier Ltd. All rights reserved.

## 1. Introduction

Sulfadiazine (SDZ) (Fig. 1(a)) is a drug used in the treatment of infections arising from Gram-positive and Gram-negative organisms, and is also administered in the treatment of toxoplasmosis (Molinoff & Ruddon, 1996; Sweetman, 2009). However, the water solubility of SDZ is low (0.074 mg/ml) and consequently reduces its bioavailability. This drug is an ampholyte, and in aqueous solutions can exist in the protonated, neutral and anionic forms as shown below (Fig. 1(a)) (Stober & DeWitte, 1982).

Cyclodextrins (CDs) (Fig. 1(b)) and some of their derivatives have been used for the molecular encapsulation of many hydrophobic and/or unstable drugs (Brewster & Loftsson, 2007; Dodziuk, 2006; Fromming & Szejtli, 1994; Laza-Knoerr, Gref, & Couvreur, 2010; Loftsson & Brewster, 2010). These, complexed drugs are typically easily wettable and more soluble, which improves their bioavailability (Brewster & Loftsson, 2007; Figueiras, Carvalho, Ribeiro, & Torres-Labandeira, 2007; Granero, Garnero, & Longhi, 2003; Klüppel Riekens et al., 2010; Wang & Cai, 2008; Yang et al., 2011).

Studies involving the complexation of SDZ with  $\beta$ -cyclodextrin and hydroxypropyl- $\beta$ -cyclodextrin have been reported in the literature (Araújo et al., 2008; Mura, Maestrelli, Cirri, Furlanetto, & Pinzauti, 2003; Zoppi, Quevedo, Delrivo, & Longhi, 2010). These

investigations have shown the feasibility of complex formation between SDZ and CDs and have demonstrated that complexation can improve the aqueous solubility of this drug. Based on these results, in the present study, we decided to focus on the preparation and physico-chemical characterization of the different complexes of SDZ with native  $\beta$ -cyclodextrin ( $\beta$ CD) and a chemically modified derivative (methyl- $\beta$ -cyclodextrin, M $\beta$ CD). Different methods were used to prepare the complexes in the solid state, including physical mixtures and freeze-drying for both CDs, as well as co-evaporation and spray-drying in the case of  $\beta$ CD alone. A complete characterization of the complexes in the aqueous solutions and solid state was determined using phase solubility analysis (PSA), nuclear magnetic resonance (NMR), differential scanning calorimetry (DSC), thermogravimetric analysis (TGA), Fourier-transform infrared spectroscopy (FT-IR), X-ray diffractometry and scanning electron microscopy (SEM). The effect of complexation on the dissolution rate of SDZ was also evaluated.

## 2. Materials and methods

### 2.1. Materials

SDZ was obtained from Parafarm (Argentina),  $\beta$ CD and M $\beta$ CD were gifts from Ferromet S.A. (agent of Roquette in Argentina). The D<sub>2</sub>O 99.9 at% D used in spectroscopic studies was purchased from Sigma®. All experiments were performed with analytical grade chemicals. The water used in these studies was generated with a Milli-Q Water Purification System (Millipore® Bedford, USA).

\* Corresponding author at: Departamento de Farmacia, Facultad de Ciencias Químicas, Universidad Nacional de Córdoba, Ciudad Universitaria, 5000 Córdoba, Argentina. Tel.: +54 351 433 4163x107; fax: +54 351 433 4163x115.

E-mail address: [mrlcor@fcq.unc.edu.ar](mailto:mrlcor@fcq.unc.edu.ar) (M.R. Longhi).

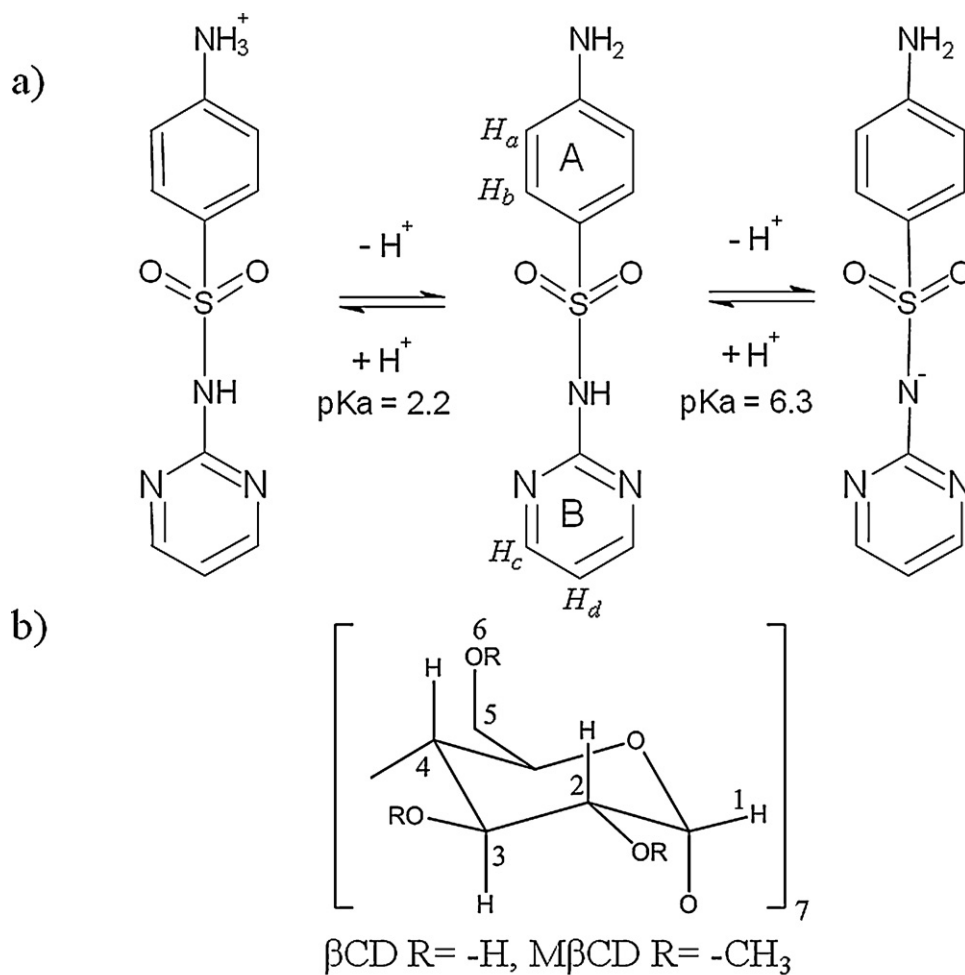


**Fig. 1.** Chemical structure and proton atom numbering scheme of: (a) SDZ (in the protonated, neutral and anionic forms) and (b)  $\beta$ -cyclodextrin and methyl- $\beta$ -cyclodextrin.

H<sub>2</sub>KPO<sub>4</sub>/HK<sub>2</sub>PO<sub>4</sub> buffer solutions of pHs 2.0 and 8.0 were also used (HI 255 Combined Meter HANNA®, USA).

## 2.2. Phase solubility analysis

The effects of each CD on the solubility of SDZ were studied according to the method described by Higuchi and Connors (1965). Excess amounts of SDZ were added to water or aqueous buffered solutions (pH 2.0 and 8.0) containing different amounts of  $\beta$ CD (0–13.2 mM) or M $\beta$ CD (0–105 mM in water and 0–85 mM in buffer solutions). Then, the resulting suspensions were sonicated in an ultrasonic bath for 1 h and placed in a 25.0 ± 0.1 °C thermostated water bath for 72 h. After equilibrium was reached, the suspensions were filtered through a 0.45  $\mu$ m membrane filter (Millipore®, USA) and analyzed by UV-vis spectrophotometry (Shimadzu UV 260 UV-vis spectrophotometer) at 264 nm. Each experiment was repeated at least three times and the results reported were the mean values. The  $K_C$  values for the corresponding SDZ:CD complexes were calculated from the slope of the phase-solubility diagrams and  $S_0$  according to (1) (Higuchi & Connors, 1965):

$$K_C = \frac{\text{slope}}{S_0(1 - \text{slope})} \quad (1)$$

The stability of the SDZ was determined in water at 25 °C, and no drug degradation was found after 72 h of incubation.

## 2.3. NMR studies

All experiments were performed on a Bruker Advance II High Resolution Spectrometer, equipped with a Broad Band Inverse probe (BBI) and a Variable Temperature Unit (VTU). The spectra were measured at 400.16 MHz and 298 K, with the chemical shift of the residual solvent at 4.8 ppm being used as an internal reference.  $\Delta\delta$  in the <sup>1</sup>H chemical shift for M $\beta$ CD and SDZ was originated from their complexation, and calculated using the following equation (2):

$$\Delta\delta = \delta_{\text{complex}} - \delta_{\text{free}} \quad (2)$$

### 2.3.1. 2D ROESY

Drug inclusion into the M $\beta$ CD cavity was studied by two-dimensional rotating frame Overhauser experiments (2D ROESY). Pulse sequence: roesygp19; 2D ROESY with cw spinlock for mixing; phase sensitive and water suppression using 3–9–19 pulse sequence with gradients; p15 (f1 channel), pulse for ROESY spinlock (200,000  $\mu$ s); d1:2 s, d19 (delay for binomial water suppression), d19=(1/(2 × d)), d=distance of next null (in Hz) use gradient ratio: gp 1:gp 2 (30:30); for z-only gradients: gpz1: 30%; gpz2: 30% use gradient files; gpnam1: SINE.100, gpnam2: SINE.100. Before Fourier transformation, the matrix was zero filled to 4096 (F2) by 2048 (F1), and Gaussian apodization functions were applied in both dimensions

#### 2.4. Preparation of the SDZ:βCD and SDZ:MβCD systems in solid state

The binary systems (SDZ:βCD or SDZ:MβCD) were prepared with equimolar ratios of SDZ with βCD or MβCD, according to the previous PSA, using the following different methods.

##### 2.4.1. SDZ:βCD and SDZ:MβCD

**2.4.1.1. Physical mixtures.** These were prepared by the simple mixing of the corresponding components using an agate mortar and pestle for 5 min to obtain a homogeneous blend at room temperature.

**2.4.1.2. Freeze-drying.** Appropriate amounts of each component were suspended in distilled water, sonicated in an ultrasonic bath at  $25.0 \pm 0.1$  °C until the drug was completely dissolved, and finally the solutions were filtered through 0.45 μm membranes (Millipore®, USA). Filtrates were frozen at  $-40$  °C for 24 h, before the freeze-drying was started (Freeze Dye 4.5 Labconco corp., Kansas City, MI).

##### 2.4.2. SDZ:βCD

**2.4.2.1. Co-evaporation.** This was prepared by dissolving and mixing equimolar amounts of SDZ and βCD in ethanol:water (1:1). The solvent was removed in vacuum after treatment with ultrasound for 1 h.

**2.4.2.2. Spray-drying.** Equimolar quantities of SDZ and βCD were dissolved in water, and the resulting solution was sonicated for 1 h. After dissolution was completed, the solution was spray dried in a Büchi Mini Spray Dryer B-290 under the following conditions: inlet temperature 119 °C, outlet temperature 38–40 °C, flow rate of the solution 120 ml/h, airflow rate 36–38 m<sup>3</sup>/h and atomizing air pressure 0.07 bar.

#### 2.5. Fourier-transform infrared spectroscopy (FT-IR)

The FT-IR spectra of pure SDZ and all binary systems obtained were measured as potassium bromide discs on a Nicolet 5 SXC FT-IR Spectrophotometer. The FT-IR spectra of SDZ:βCD and SDZ:MβCD complexes were compared with their physical mixtures and pure SDZ and CDs.

#### 2.6. Differential scanning calorimetry (DSC) and thermogravimetric analysis (TG)

Differential scanning calorimetry (DSC) measurements of the pure materials and binary systems were carried out using a DSC TA 2920. The thermal behavior was studied by heating the 1–3 mg samples in aluminum-pin-hole pans to 25–350 °C, at a rate of 10 °C/min and under a nitrogen flow.

The TG curves of the different samples were obtained using a TG TA 2950 under the same conditions as those of DSC. Data were processed using the TA Instruments Universal Analysis 2000 software.

#### 2.7. Powder X-ray diffraction studies

The powder X-ray diffraction patterns were obtained with a Philips X'Pert PRO PANalytical powder diffractometer (Philips®, The Netherlands), using Ni-filtered Cu Kα radiation at 40 kW, 40 mA and a scan rate of 0.02°/min. The diffractograms were recorded from 5° to 50° (2θ).

#### 2.8. Scanning electron microscopy studies

The microscopic morphological structures of the raw materials, complexes and physical mixtures were investigated and photographed using a scanning electron microscope LEO Model EVO 40XVP. The samples were fixed on a brass stub using double-sided aluminum tape, which were then made electrically conductive by being gold coated in vacuum using a PELCO Model 3 sputter coater. The magnification selected was sufficient to be able to appreciate in detail the general morphology of the samples under study.

#### 2.9. Dissolution rate studies

The dissolution rate studies of SDZ (alone and from SDZ:βCD systems) were conducted in a dissolution apparatus (Hanson SR11 6 Flask Dissolution Test Station, Hanson Research Corporation, Chatsworth, USA) using the paddle method according to USP XXX, at  $37 \pm 0.5$  °C and stirring at 75 r/min. 42 mg of SDZ or its equivalent amount of SDZ:βCD was added to 250 ml of diluted hydrochloric acid (0.1 M), and aliquots of the dissolution medium (2 ml) were taken at suitable time intervals. The withdrawn samples were then replaced by equal volumes of fresh dissolution medium maintained at the same temperature. Each solution was diluted and determined spectrophotometrically (Shimadzu UV-Mini 1240 spectrophotometer) at 243 nm. The data from the release of SDZ were analyzed using the similarity factor ( $f_2$ ) (US Department of Health and Human Services, 1997) by considering the free drug as reference and the quantity of drug released at different time intervals. The similarity factor ( $f_2$ ) (3) is a logarithmic reciprocal square root transformation of the sum of the squared error and is used as a measurement of the similarity by considering the percentage (%) dissolution between the two curves, and is expressed as:

$$f_2 = 50 \log \left\{ \left[ 1 + \frac{1}{n} \sum_{t=1}^R (R_t - T_t)^2 \right]^{-0.5} \right\} \times 100 \quad (3)$$

### 3. Results and discussion

#### 3.1. Phase solubility analysis

As discussed above, SDZ is an ampholyte, and depending on the pH of the aqueous solutions, it can exist in the protonated, neutral or anionic forms. In order to determine the influence of drug ionization on its affinity for βCD and MβCD, phase-solubility diagrams (PSD) were determined at three different pHs (pH 2 protonated, pH 6 neutral and pH 8 anionic drug form).

The effect of drug ionization on the solubility of its complexes with βCD and MβCD is shown in Fig. 2. The SDZ:βCD and SDZ:MβCD isotherms were linear within the CD concentration ranges studied and corresponded to A<sub>L</sub>-type profiles, with slope values less than unity indicating the occurrence of soluble complexes of 1:1 mol/mol stoichiometries for both CDs and SDZ of protonated (pH 2), neutral (pH 6) and anionic (pH 8) forms. The corresponding affinity constant ( $K_C$ ), intrinsic solubility ( $S_0$ ), maximum solubility ( $S_{max}$ ) and efficiency of solubility ( $ES$ ,  $S_{max}/S_0$ ) values were calculated from each PSD and are presented in Table 1.

The  $K_C$  values obtained demonstrated that the binding of SDZ with MβCD was relatively lower than that with βCD. This behavior was probably be due to the presence of the substituent methyl groups at the rims of the MβCD, which may have caused a steric hindrance to the inclusion of the drug. On analyzing the effects of pH, it can be observed that the values of  $K_C$  for the complexes with both βCD and MβCD were higher in water. This result may be due to SDZ being present as a neutral species in water, which is favorable for complex formation. However, the efficiency of the solubility

**Table 1**Data of the phase solubility studies of SDZ with  $\beta$ CD and M $\beta$ CD.

Systems	Solvent	pH	$K_C$	$S_0$ (mg/ml)	$S_{max}$ (mg/ml)	ES
SDZ: $\beta$ CD	Water pH 6 <sup>a</sup>	5.96	282 $\pm$ 15	0.073 $\pm$ 0.009	0.33 $\pm$ 0.02	4
	Buffer pH 2	1.74	131.7 $\pm$ 0.3	0.18 $\pm$ 0.04	0.50 $\pm$ 0.02 <sup>b</sup>	3
	Buffer pH 8	7.65	55 $\pm$ 2	0.90 $\pm$ 0.06	1.54 $\pm$ 0.03 <sup>b</sup>	2
SDZ:M $\beta$ CD	Water pH 6	5.63	243 $\pm$ 6	0.073 $\pm$ 0.009	1.90 $\pm$ 0.03 <sup>c</sup>	26
	Buffer pH 2	1.96	149 $\pm$ 3	0.18 $\pm$ 0.04	2.29 $\pm$ 0.02 <sup>d</sup>	13
	Buffer pH 8	7.62	44 $\pm$ 2	0.90 $\pm$ 0.06	3.566 $\pm$ 0.008 <sup>d</sup>	4

<sup>a</sup> Zoppi et al. (2010).<sup>b</sup> SDZ solubility in  $\beta$ CD (13.2 mM) solutions.<sup>c</sup> SDZ solubility in M $\beta$ CD (105 mM) solutions.<sup>d</sup> SDZ solubility in M $\beta$ CD (85 mM) solutions.

was higher in aqueous buffered solutions, because of the combined effect of the complex formation and the existence of the drug as an ionized species. It is also possible to observe that at pH 2, where the drug was in its protonated form, the  $K_C$  values were greater than at pH 8. This might be attributed to the fact that the amine function in ring A was oriented towards the bulk solvent, while for the drug is in anionic form, the negative charge was positioned in the middle of the SDZ molecule, thereby producing an unfavorable effect for complexation. Finally, it should be noted that while the SDZ:M $\beta$ CD systems presented low  $K_C$  values compared with those containing  $\beta$ CD (with the exception of the aqueous buffered solutions of pH 2), the increase in the solubility of the drug was higher because it was possible to add larger amounts of M $\beta$ CD due to its superior aqueous solubility.

### 3.2. NMR studies

#### 3.2.1. <sup>1</sup>H NMR experiments

NMR proton spectroscopy is a frequently used analytical tool to study the inclusion of guest molecules into a host (Fromming & Szejtli, 1994). The inclusion of SDZ into the M $\beta$ CD cavity was first evaluated by the changes in the chemical shifts ( $\delta$ ) of the protons in the complex, relative to the free SDZ and M $\beta$ CD (Fig. 3(A and B)). Tables 2 and 3 present the assignments of the SDZ and M $\beta$ CD peaks and the chemical shift deviations due to complexation (see proton numbering in Fig. 1).

It can be seen that the protons lying in the interior of the hydrophobic cavity of M $\beta$ CD ( $H_3$  and  $H_5$ ) exhibited displacements in their  $\delta$  in the presence of the drug, thus confirming the formation of an inclusion complex. For the SDZ:M $\beta$ CD complex, a deshielding and a shielding displacement was found for  $H_5$  and  $H_3$ , respec-

**Table 2**

Chemical shifts for the protons of SDZ in the free and complex states.

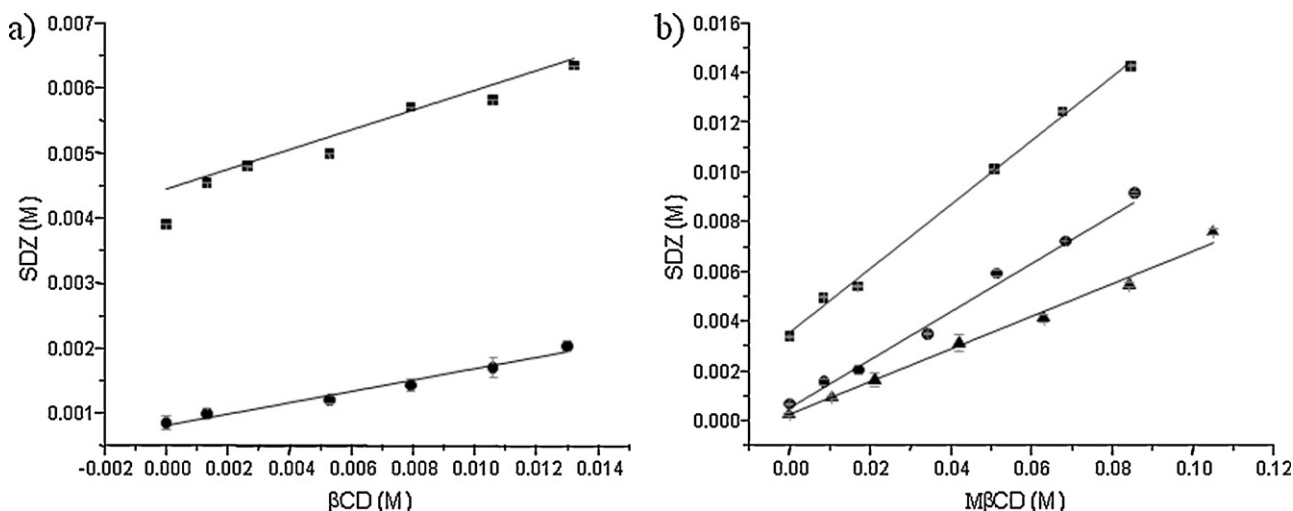
Proton	$\delta_0$	$\delta_c$	$\Delta\delta$
SDZ			
$H_a$	6.7284	6.5713	-0.1571
$H_b$	7.5882	7.7470	0.1588
$H_c$	8.2308	8.5522	0.3214
$H_d$	6.7801	7.1435	0.3634

**Table 3**Chemical shifts for the protons of M $\beta$ CD in the free and complex states.

Proton	$\delta_0$	$\delta_c$	$\Delta\delta$
M $\beta$ CD			
$H_{1s}$	5.2815	5.2596	-0.0219
$H_{1us}$	5.0880	5.0749	-0.0131
$H_{3us}$	4.0369	4.0085	-0.0284
$H_{3s}$	3.9591	3.9287	-0.0304
$H_4-H_{2us}$		Overlapped	
$H_6$	3.8898	3.8706	-0.0192
$H_5$	3.7849	3.8088	0.0239
$H_{2s}$	3.4111	3.3925	-0.0186
$CH_3$	3.5806	3.5681	-0.0125

s, substituted; us, unsubstituted.

tively, which may have resulted from the partial inclusion of an electronegative functional group that produced a deshielding effect on  $H_5$ . In addition, the  $\delta$  corresponding to the protons located at the outer surface of M $\beta$ CD ( $H_1$ ,  $H_2$  and  $H_4$ ) were also modified, which might have been due to a conformational rearrangement in the host molecule.

**Fig. 2.** Phase-solubility diagrams of: (a) SDZ: $\beta$ CD in buffer solutions pH 8.0 (■), and pH 2.0 (●), (b) SDZ:M $\beta$ CD in water (▲), in buffer solutions pH 8.0 (■), and pH 2.0 (●).

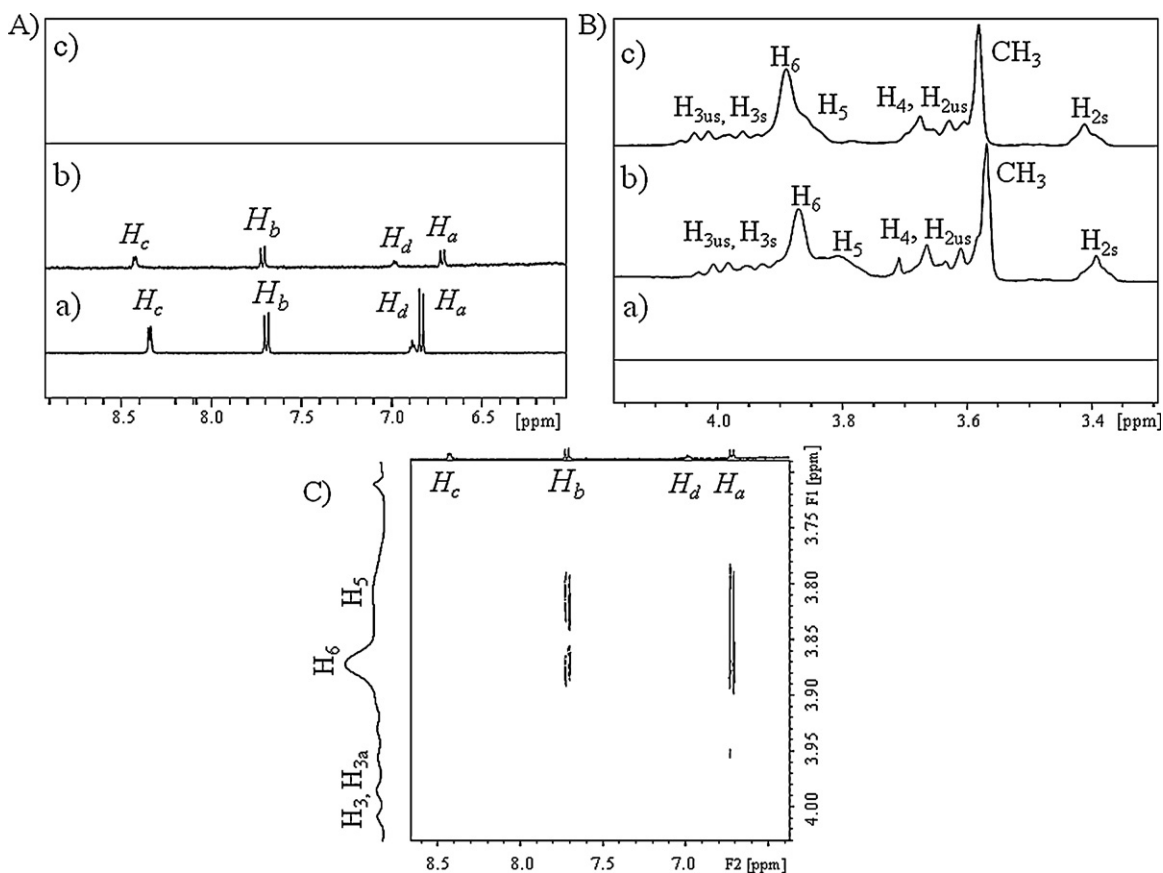


Fig. 3. (A and B)  $^1\text{H}$  NMR Spectra of (a) SDZ, (b) SDZ:M $\beta$ CD system, and (c) M $\beta$ CD. (C) Partial contour plot of the 2D ROESY spectrum of the SDZ:M $\beta$ CD system.

For SDZ, deshielding effects were observed for H<sub>b</sub>, H<sub>c</sub> and H<sub>d</sub>, probably arising from van der Waals interactions between SDZ and M $\beta$ CD, suggesting the deep insertion of this molecule into the M $\beta$ CD cavity.

### 3.2.2. ROESY experiments

2D ROESY experiments were carried out to investigate the inclusion of SDZ into the M $\beta$ CD cavity. Fig. 3(C) shows partial contour plots of 2D ROESY spectra for the studied system. Here, it can be observed that the H<sub>a</sub> and H<sub>b</sub> protons of SDZ correlated with the inner protons of M $\beta$ CD (H<sub>5</sub> and H<sub>6</sub>), indicating the formation of an inclusion complex in which the ring A of SDZ was deeply inserted into the hydrophobic cavity of the host. The results obtained by the NMR techniques showed good correlations with those observed for the SDZ: $\beta$ CD complex presented in our previous work (Zoppi et al., 2010).

### 3.3. Fourier-transform infrared spectroscopy

FT-IR spectroscopy was used to assess the interaction between both CDs and SDZ in the solid state, due to the changes occurring in the spectrum by complexation. The binary complexes were examined and compared with pure SDZ,  $\beta$ CD and M $\beta$ CD and the corresponding physical mixtures (Fig. 4). Characteristic bands of SDZ (Fig. 4(a)) were found at 3450 and 3410  $\text{cm}^{-1}$  (N–H symmetric stretching); 1650  $\text{cm}^{-1}$  (NH<sub>2</sub> deformation); 1580, 1490, 1440 and 1410  $\text{cm}^{-1}$  (ring skeletal vibrations); 1325  $\text{cm}^{-1}$  (SO<sub>2</sub> asymmetric stretching) and 1155  $\text{cm}^{-1}$  (symmetric stretching) (Stober & DeWitte, 1982). The spectra of the physical mixtures with  $\beta$ CD and M $\beta$ CD consisted of an overlay of the pure compound spectra (Fig. 4(c) and (h)).

In contrast, the FT-IR spectra of the complexes prepared by the freeze-drying, spray-drying and co-evaporation methods (Fig. 4(d), (e), (f), and (i)) did not reveal any new bands. Nevertheless, although no new chemical bonds were formed, the complexes showed some differences compared to pure SDZ. The band at 1650  $\text{cm}^{-1}$  corresponding to NH<sub>2</sub> deformation became broader and the bands corresponding to the ring skeletal vibrations presented important changes. These results confirm the existence of intermolecular interactions between SDZ and both CDs in the solid state.

### 3.4. Differential scanning calorimetry and thermogravimetric analysis

DSC and TG are frequently the pharmaceutical thermal analysis techniques of choice for studying complexation, due to their ability to provide detailed information about both the physical and energetic properties of substances (Clas, Dalton, & Hancock, 1999). The DSC and TG curves of pure components and binary systems from the present study are shown in Fig. 5 (A and B, respectively). The thermal curve of SDZ was typical of a crystalline anhydrous substance, with a sharp endothermic event occurring at 263.2  $^{\circ}\text{C}$ , corresponding to the melting point of the drug, followed by an exothermic event attributable to its thermal decomposition, as can be observed by comparison with the TG curve. Both  $\beta$ CD and M $\beta$ CD lost water at temperatures between 25 and 100  $^{\circ}\text{C}$ , with decomposition taking place above 300  $^{\circ}\text{C}$  as evidenced by the mass loss observed in the TG curves.

On analyzing the physical mixtures of SDZ: $\beta$ CD and SDZ:M $\beta$ CD, the same characteristic events observed for the pure compounds were found. Therefore, no inclusion complexes were obtained. However, in the solid obtained by co-evaporation, a thermal event

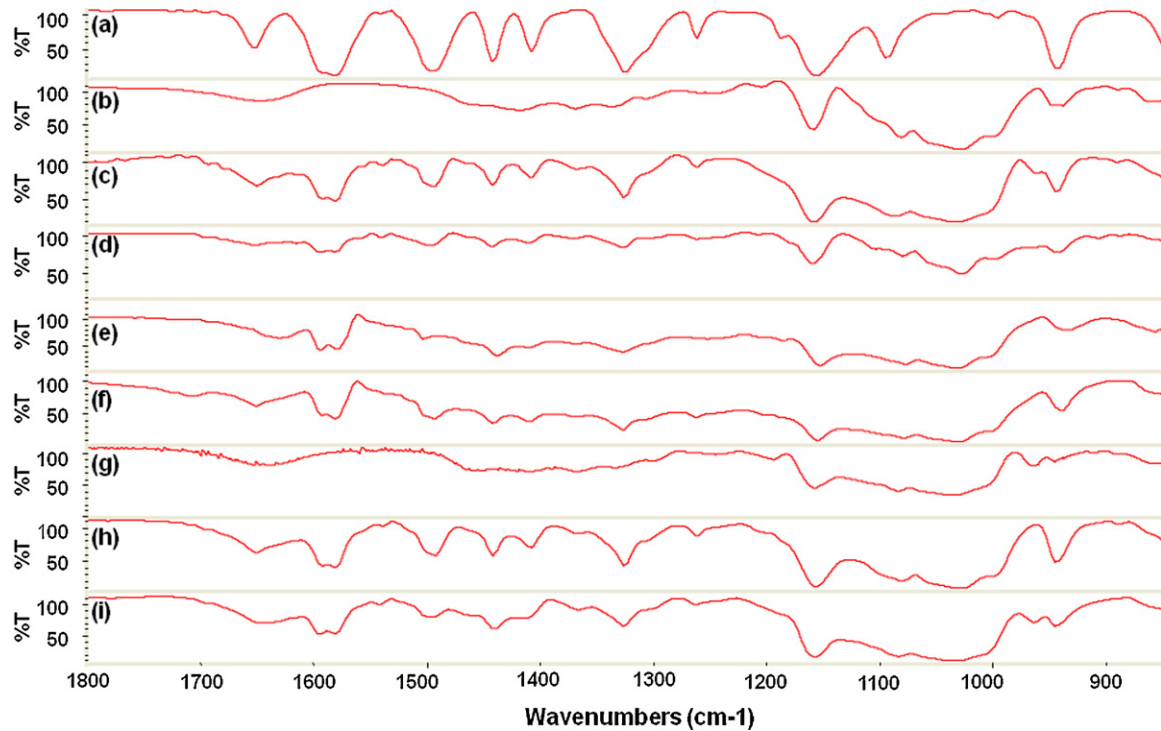


**Fig. 4.** IR spectra of: (a) SDZ, (b)  $\beta$ CD, (c) SDZ: $\beta$ CD physical mixture system, (d) SDZ: $\beta$ CD freeze-dried system, (e) SDZ: $\beta$ CD spray-dried system, (f) SDZ: $\beta$ CD co-evaporation system, (g) M $\beta$ CD, (h) SDZ:M $\beta$ CD physical mixture system, and (i) SDZ:M $\beta$ CD freeze-dried system.

corresponding to the melting point of SDZ can be seen, indicating a weak interaction between the drug and  $\beta$ CD for this system. In addition, the disappearance of the SDZ melting point in the freeze-dried products with both CDs and in the spray-dried product with  $\beta$ CD, suggests the formation of true inclusion complexes using these two methods.

### 3.5. Powder X-ray diffraction studies

The powder X-ray diffraction patterns of SDZ,  $\beta$ CD, M $\beta$ CD and the binary systems are shown in Fig. 6. The diffractogram of SDZ exhibited a series of intense and sharp peaks, at diffraction angles ( $2\theta$ ) of 7.2, 11.9, 13.0, 14.3, 16.7, 19.2, 21.5, 23.0, 23.5, 26.1, 29.5, 36.2 and 43.7°, demonstrating the crystalline nature of the drug.

The diffraction pattern obtained for  $\beta$ CD also showed that it was a crystalline substance, because of the presence of characteristic peaks at diffraction angles ( $2\theta$ ) of 9.0, 10.9, 12.5, 12.7, 14.7, 17.7, 19.8, 22.7, 24.5, 27.0, 32.0 and 34.8°. It was possible to observe the presence of all of the principal peaks of SDZ and  $\beta$ CD in the diffractograms of the SDZ: $\beta$ CD systems prepared by physical mixture and co-evaporation, although at a lower intensity due to the dilution of the raw materials. In contrast, in the SDZ: $\beta$ CD complex obtained by freeze-drying, a decrease in the crystallinity degree could be observed, although some characteristic SDZ peaks were still detectable. Finally, a total drug amorphization was induced by the spray-dried system.

The X-ray diffraction pattern of M $\beta$ CD revealed that it was an amorphous substance. For the SDZ:M $\beta$ CD systems prepared

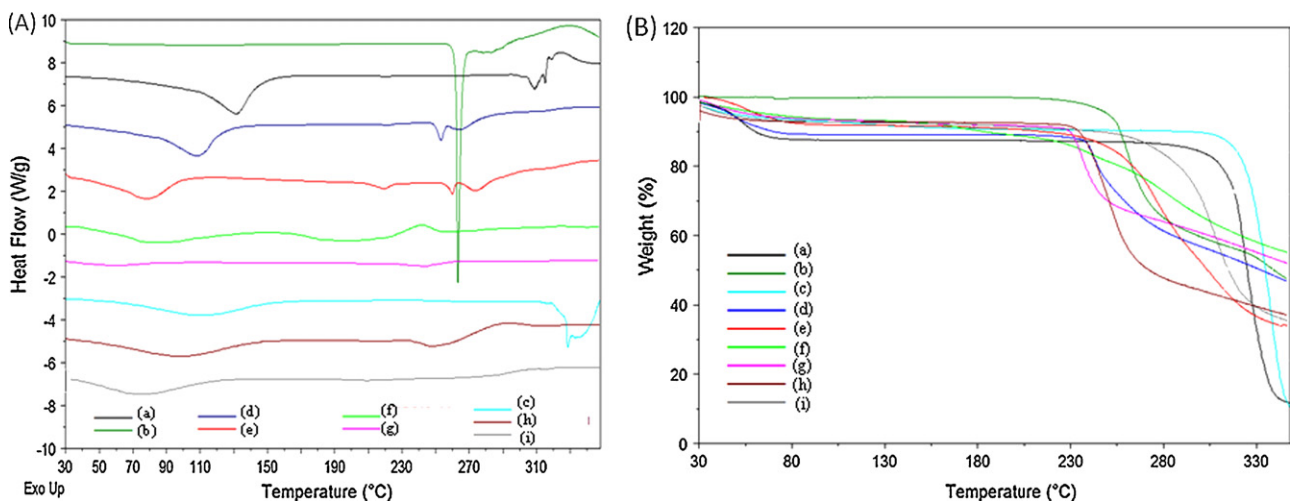


**Fig. 5.** DSC (A) and TG (B) curves of: (a)  $\beta$ CD, (b) SDZ, (c) M $\beta$ CD, (d) SDZ: $\beta$ CD physical mixture system, (e) SDZ: $\beta$ CD co-evaporation system, (f) SDZ: $\beta$ CD freeze-dried system, (g) SDZ: $\beta$ CD spray-dried system, (h) SDZ:M $\beta$ CD physical mixture system, and (i) SDZ:M $\beta$ CD freeze-dried system.

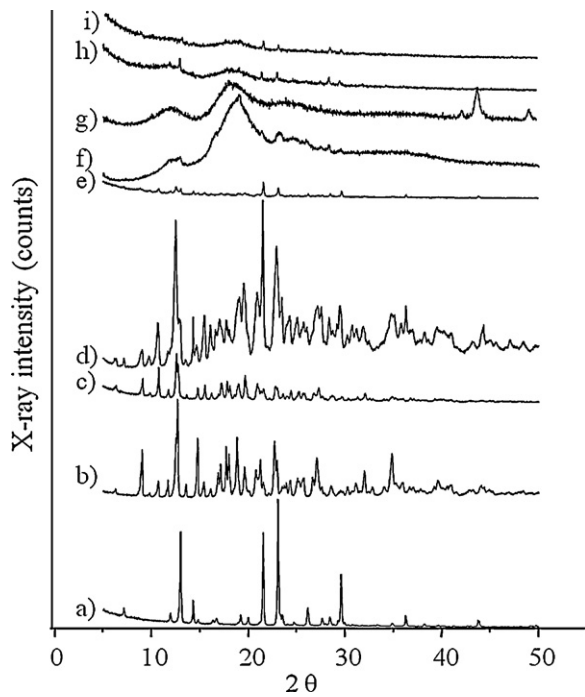


**Fig. 6.** X-ray diffractograms of: (a) pure SDZ, (b) pure βCD, (c) SDZ:βCD physical mixture system, (d) SDZ:βCD co-evaporation system, (e) SDZ:βCD freeze-dried system, (f) SDZ:βCD spray-dried system, (g) pure MβCD, (h) SDZ:MβCD physical mixture system, (i) SDZ:MβCD freeze-dried system.

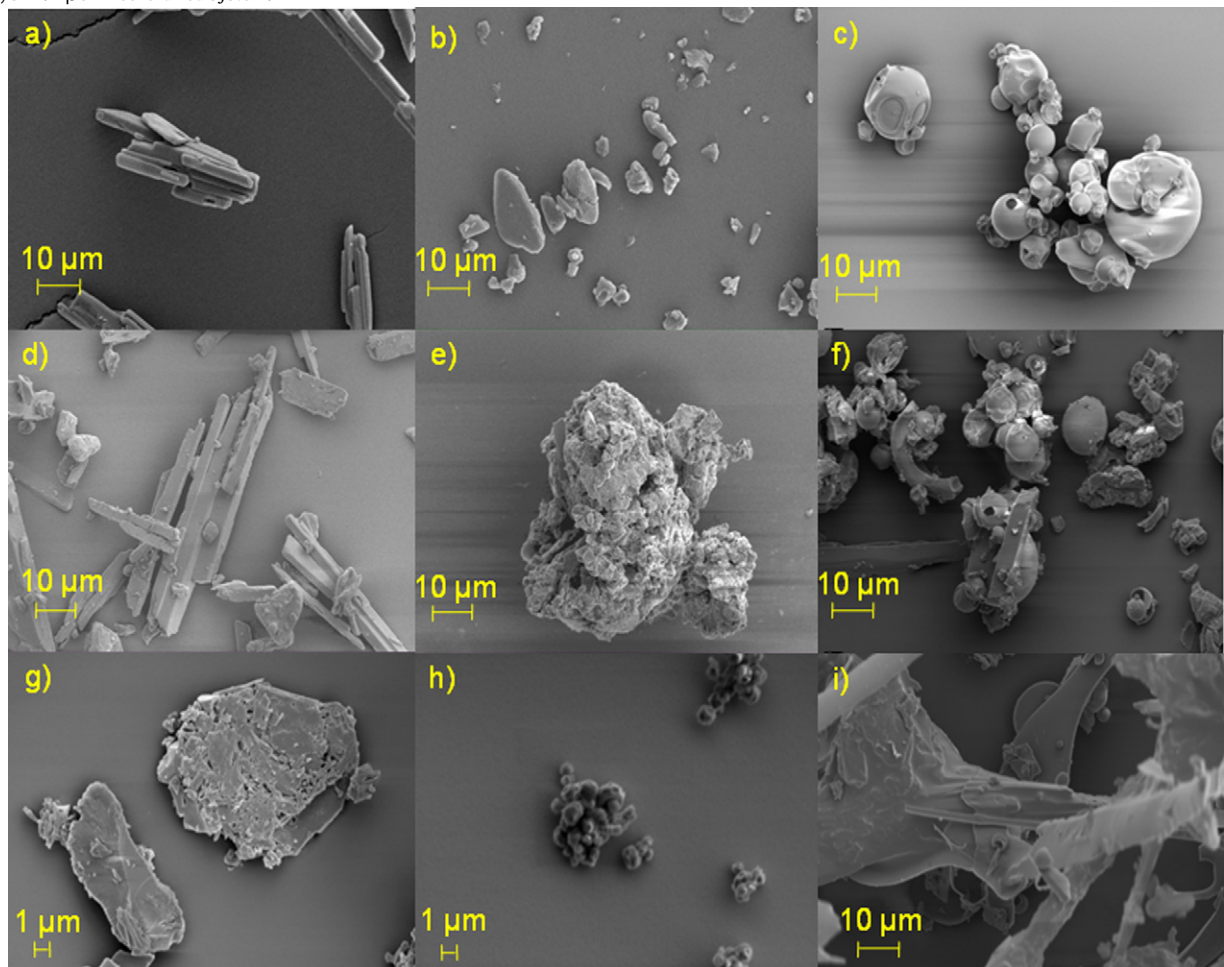


**Fig. 7.** Scanning electron microphotographs of (a) SDZ, (b) βCD, (c) MβCD, (d) SDZ:βCD physical mixture system, (e) SDZ:βCD freeze-dried system, (f) SDZ:MβCD physical mixture system, (g) SDZ:βCD co-evaporation system, (h) SDZ:βCD spray-dried system, and (i) SDZ:MβCD freeze-dried system.

by physical mixture and freeze-drying, it was possible to observe a severe decrease in the crystallinity degree of these solids. The results obtained by DSC and powder X-ray diffraction revealed the production of a low crystallinity state in the drug:cyclodextrin products prepared by the freeze-dried and spray-dried methods as a consequence of host–guest solid-state interactions, indicative of the possible formation of an inclusion complex.

### 3.6. Scanning electron microscopy

In Fig. 7, the SEM images of SDZ, βCD, MβCD and the binary systems are shown.

SDZ was present as rectangular crystals of irregular sizes. βCD exhibited a parallelogram shape and MβCD being composed of spherical particles of an amorphous character. The physical mixtures SDZ:βCD and SDZ:MβCD (Fig. 7(d) and (f)) showed particles of CDs embedded with SDZ and morphologies comparable with those of the pure compounds, revealing no apparent interaction between the species in the solid state. In contrast, a change in the morphology and shape of the particles was observed in the freeze-dried products of βCD and MβCD, demonstrating an apparent interaction in the solid state (Fig. 7(e) and (i)), which might be indicative of the presence of a new solid phase. However, in the case of the SDZ:βCD system prepared by spray drying (Fig. 7(h)), the original morphology of the raw materials disappeared, and therefore it was not possible to differentiate individual components. The spray-dried product showed amorphous and homogeneous aggregates

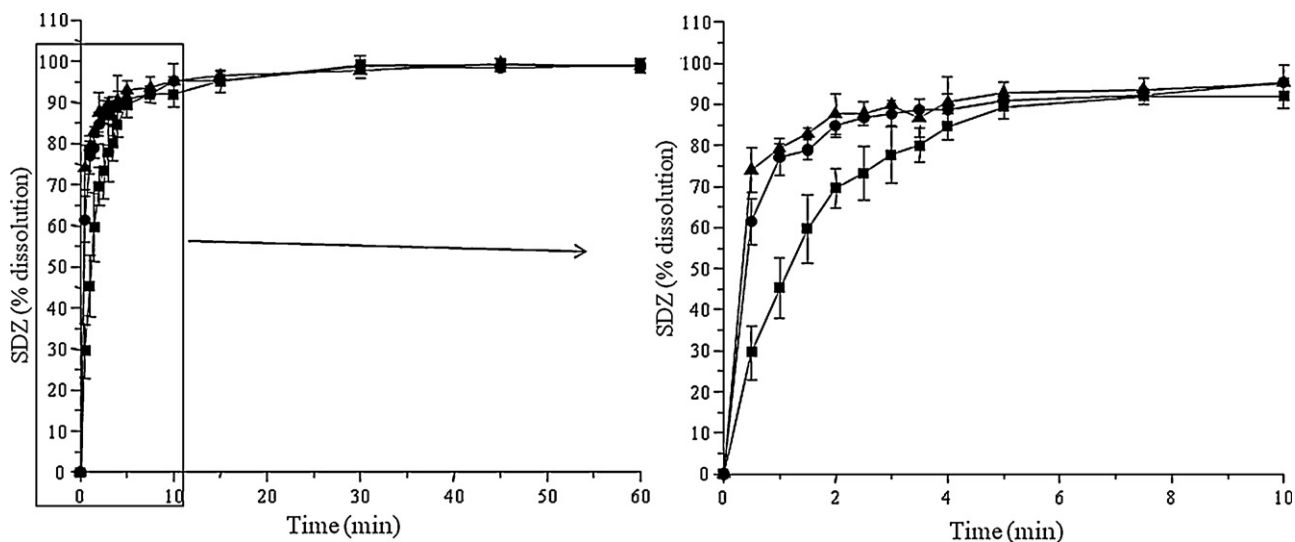


Fig. 8. Dissolution rate profiles for SDZ (■), SDZ- $\beta$ CD physical mixture (●) and freeze-dried complex SDZ- $\beta$ CD (▲).

of spherical particles, which is a characteristic aspect of this type of systems. Finally, in the microphotographs of the system prepared by co-evaporation (Fig. 7(g)), the presence of particles of pure components mixed with particles of different morphologies can be observed, which may be attributed to incomplete complex formation. In conclusion, the drastic changes in particle shape and the appearance of spray-dried and freeze-dried products are indicative of the presence of new solid phases.

### 3.7. Dissolution studies

The selection of the system used to carry out the dissolution studies was based on a future possible production on an industrial scale. The SDZ: $\beta$ CD complex was chosen because  $\beta$ CD has a better solubilization effect than M $\beta$ CD (at the same concentration) in addition to having a lower cost. For the method of preparation, freeze-drying was chosen due to it being the most frequently used on an industrial scale, and it was also compared with the system prepared by physical mixture and with the drug by itself (Fig. 8). It was evident that both binary systems exhibited a faster dissolution rate than the free drug. Then, to analyze dissolution data equivalence, a model independent approach based on the calculation of the similarity factor ( $f_2$ ) was used. For curves to be considered equivalent, the  $f_2$  values should be close to 100, and values greater than 50 (50–100) ensure similarity of the two curves. In this study the values obtained were 34.5% and 28.8% for the products obtained by physical mixture and freeze-drying, respectively. These results indicate that the curves of the binary systems were not similar to the curve of the drug alone, implying that the presence of  $\beta$ CD caused an enhancement of the SDZ dissolution rate. The effect observed for the system prepared by freeze-drying may be attributed to an increase in solubility due to complexation and also to the low crystalline state of the drug that was already confirmed by DSC and X-ray diffraction studies. In the case of the physical mixture, the improvement of the SDZ dissolution rate may have been due to an in situ inclusion process that produced an increase in the amount of the dissolved drug.

## 4. Conclusions

Using complexation with cyclodextrins ( $\beta$ CD and M $\beta$ CD), the aqueous solubility of SDZ was improved substantially. Moreover, it was possible to obtain a greater overall solubility through a

combined approach of pH adjustment and complexation with CDs. The results obtained from FT-IR, DSC, TG, X-ray diffraction and SEM studies showed that inclusion complexes could be obtained in solid state with both cyclodextrins. Particles of the complex prepared by the freeze-dried and spray-dried methods showed a distinctive morphology from the ones observed in the raw materials. Taking into account the results obtained in this investigation, we can postulate that the interaction of SDZ and CDs, through the formation of inclusion complexes, leads to important modifications in the physicochemical properties of the guest molecule, which undoubtedly has a positive effect on the biological properties, such as an improvement in the SDZ bioavailability. This might eventually have relevant pharmaceutical applications in the preparation of an oral dosage form containing SDZ.

In addition, the results obtained at different pH values, also provide interesting alternatives for the preparation of ternary complexes between SDZ, CDs and amino acids, which may produce a better effect on the solubility of the drug. This line of investigation has already been commenced by our research group.

## Acknowledgments

The authors thank the Fondo para la Investigación Científica y Tecnológica (FONCYT) Préstamo BID PICT 1376, the Secretaría de Ciencia y Técnica de la Universidad Nacional de Córdoba (SECyT), and the Consejo Nacional de Investigaciones Científicas y Tecnológicas de la Nación (CONICET) for financial support. We also thank Ferromet S.A. (agent of Roquette in Argentina) for its donation of  $\beta$ -cyclodextrin and methyl- $\beta$ -cyclodextrin. We are grateful to Dr. Gloria Bonetto for NMR measurements and for her helpful discussion of the  $^1\text{H}$  NMR spectra, and Dr. Paul Hobson, native English speaker, for revision of the manuscript.

## References

- Araújo, M. V. G., De, Vieira, E. K. B., Silva Lázaro, G., Conegero, L. S., Almeida, L. E., Barreto, L. S., et al. (2008). Sulfadiazine/hydroxypropyl- $\beta$ -cyclodextrin host-guest system: Characterization, phase-solubility and molecular modeling. *Bioorganic Medical Chemistry*, 16, 5788–5794.
- Brewster, M. E. & Loftsson, T. (2007). Cyclodextrins as pharmaceutical solubilizers. *Advanced Drug Delivery Reviews*, 59, 645–666.
- Clas, S. D., Dalton, C. R. & Hancock, B. C. (1999). Differential scanning calorimetry: Applications in drug development. *Pharmaceutical Science and Technology Today*, 2, 311–320.
- Dodziuk, H. (2006). *Cyclodextrins and their complexes: Chemistry, analytical methods, applications*. Weinheim: Wiley-VCH Verlag GmbH & Co., KGaA.



- Figueiras, A., Carvalho, R. A., Ribeiro, L., Torres-Labandeira, J. J. & Veiga, F. J. B. (2007). Solid-state characterization and dissolution profiles of the inclusion complexes of omeprazole with native and chemically modified  $\beta$ -cyclodextrin. *European Journal of Pharmaceutics and Biopharmaceutics*, 67, 531–539.
- Fromming, K. H. & Szejtli, J. (1994). *Cyclodextrins in pharmacy*. Dordrecht, The Netherlands: Kluwer Academic Publishers.
- Granero, G. E., Garnero, C. & Longhi, M. R. (2003). The effect of pH and triethanolamine on sulfisoxazole complexation with hydroxypropyl- $\beta$ -cyclodextrin. *European Journal of Pharmaceutical Sciences*, 20, 285–293.
- Higuchi, T. & Connors, K. (1965). Phase solubility techniques. In C. Reilly (Ed.), *Advances in analytical chemistry and instrumentation*. (pp. 117–212). New York: Wiley Interscience.
- Klüppel Riekes, M., Piazzon Tagliari, M., Granada, A., Kuminek, G., Segatto Silva, M. A. & Stulzer, H. K. (2010). Enhanced solubility and dissolution rate of amiodarone by complexation with  $\beta$ -cyclodextrin through different methods. *Materials Science and Engineering C*, 30, 1008–1013.
- Laza-Knoerr, A. L., Gref, R. & Couvreur, P. (2010). Cyclodextrins for drug delivery. *Journal of Drug Targeting*, 18, 645–656.
- Loftsson, T. & Brewster, M. E. (2010). Pharmaceutical applications of cyclodextrins: Basic science and product development. *Journal of Pharmacy and Pharmacology*, 62, 1607–1621.
- Molinoff, P. B. & Ruddon, R. W. (1996). *Goodman and Gilman's: The pharmacological basis of therapeutics*. (9th ed.). New York: Pergamon Press.
- Mura, P., Maestrelli, F., Cirri, M., Furlanetto, S. & Pinzauti, S. (2003). Differential scanning calorimetry as an analytical tool in the study of drug-cyclodextrin interactions. *Journal of Thermal Analysis and Calorimetry*, 73, 635–646.
- Stober, H. & DeWitte, W. (1982). Sulfadiazine. In K. Florey (Ed.), *Analytical profiles of drug substances* (pp. 523–551). New York: Academic Press.
- Sweetman, S. C. (2009). *Martindale: The Complete Drug Reference* (36 ed.). London: Pharmaceutical Press.
- US Department of Health and Human Services, FDA, CDER. (1997). Guidance for Industry. Dissolution testing of immediate release solid oral dosage forms.
- Wanga, J. & Cai, Z. (2008). Investigation of inclusion complex of miconazole nitrate with  $\beta$ -cyclodextrin. *Carbohydrate Polymers*, 72, 255–260.
- Yang, L., Chen, W., Ma, S. X., Gao, Y. T., Huang, R., Yan, S. J., et al. (2011). Host-guest system of taxifolin and native cyclodextrin or its derivative: Preparation, characterization, inclusion mode, and solubilization. *Carbohydrate Polymers*, 85, 629–637.
- Zoppi, A., Quevedo, M. A., Delrivo, A. & Longhi, M. R. (2010). Complexation of sulfonamides with  $\beta$ -cyclodextrin studied by experimental and theoretical methods. *Journal Pharmaceutical Sciences*, 99, 3166–3176.